Environmental Impact Optimisation of Flight Plans in a Fixed and Free Route network

Vergnes, Florent; Bedouet, Judicaël; Olive, Xavier; Sun, Junzi

Publication date
2022

Document Version
Final published version

Published in
10th International Conference for Research in Air Transportation

Environmental Impact Optimisation of Flight Plans in a Fixed and Free Route network

Florent Vergnes*†, Judicaël Bedouet*, Xavier Olive*, Junzi Sun‡

*ONERA – DTIS
Université de Toulouse
Toulouse, France

†École Nationale de l'Aviation Civile
Université de Toulouse
Toulouse, France

‡Faculty of Aerospace Engineering,
Delft University of Technology,
Delft, the Netherlands

***Abstract*—Efforts to minimise the environmental impact of aviation can be implemented at several levels including electric green taxiing systems, novel propulsion systems, jet fuels, improvements in aircraft efficiency and optimisation of climb profiles. In this paper, we address the optimisation of flight plans in a route network considering operational parameters and weather forecast. We implement an A* based approach to explore all possible sequences of nodes, altitudes with given wind, temperature and pressure forecasts in order to minimise total flown distance, total burnt fuel, CO_2 and non-CO_2 emissions, the latter being responsible for two-thirds of aviation radiative forcing. We evaluated our approach on both a network of standard routes and through free route areas, and observed that our optimised flight plans are consistent with those that have actually been filed to be flown in similar weather conditions during December 2021.**

***Keywords* —** flight plan optimisation; environmental impact; green aviation; graph optimisation

I. Introduction

Global population growth, economical growth rate as well as technological evolution favour a thriving air transport industry. Currently, aviation is responsible for about 3–5% of total global warming [1]. The aviation-induced climate impact consists of carbon dioxide (CO_2) emissions and of non-CO_2 effects. The non-CO_2 effects comprise nitrogen oxide (NO_X) emissions that are causing a concentration change in ozone and methane, water vapour emissions, aerosols, and persistent contrail and contrail-cirrus formation. CO_2 and non-CO_2 effects induce a change in the Earth's radiation balance between incoming solar radiation and thermal outgoing radiation.

Recently, there have been various approaches to mitigate aviation's climate impact with different propulsion techniques, including electric propulsion, battery storage and hydrogen aircraft; with trajectory optimisation techniques [2] or by modifying aircraft maneuvers to avoid areas where non CO_2 effects would be enhanced [3], [**?**].

In this contribution, we address the problem of the generation of flight plans aiming at minimising the climate impact of the trajectory expected to be flown. Considered metrics include the total burnt fuel, estimated with the BADA model [4], then CO_2 and non-CO_2 emissions estimated with OpenAP [5]. Flight plans are defined as a sequence of waypoints linking a departure to an arrival airports. Historically, waypoints are connected by airways forming the ATS route network (ARN). The first waypoint of a flight plan is usually labelled with an altitude (in Flight Level FL) and an airspeed (in knots, or occasionally in Mach number), but these parameters may be redefined along the route.

This network structure naturally leads to shortest path algorithms in graphs, and we present a particular implementation of the A* algorithm with a heuristic to preselect nodes to be expanded. In a second stage, the approach is adapted to the specificities of Free Route Areas (FRA), which cover a major part of Europe, in December 2021, (Figure 1). In FRA, aircraft are still expected to fly over (or fly by) predefined waypoints, but those are no longer connected by airways, only `DIRECT` instructions. This system is more flexible and cost-effective from the aircraft point of view but requires extra preparation from the Air Traffic Control (ATC) perspective.

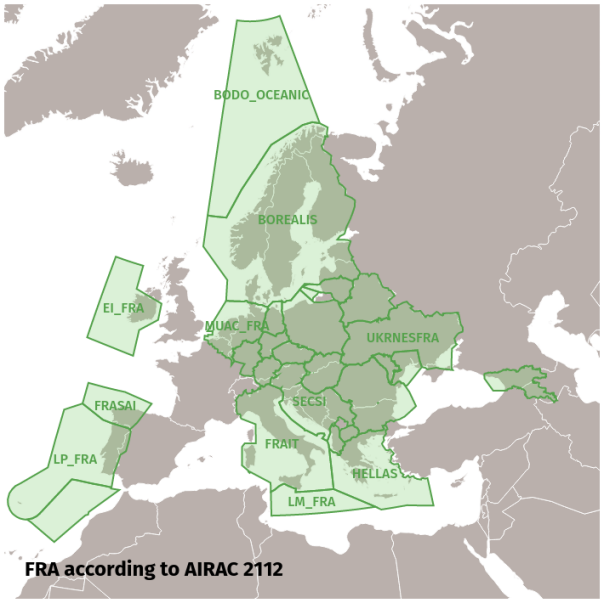

Fig. 1. Free route areas (FRA) defined in AIRAC 2112

Flight plan optimisation naturally relates to the wider topic of trajectory optimisation, which is defined as the process of determining the best possible trajectory of a dynamical system (an aircraft in our case) in a finite dimension space with respect to some user defined objectives and constraints. Chai et al. [2] survey a wide range of techniques to address this problem.

The most reliable technique is based on optimal control: it works in continuous time, considers the system's dynamical behaviour (differential equations) to efficiently simulate, predict and optimise the trajectory of aircraft. This optimisation problem can be solved analytically or numerically, for example with Dynamic Programming or Non-Linear Programming [6], [7].

A different way to address the dynamic optimisation problem is to simplify the equations of aircraft dynamics and to consider discrete optimisation techniques like geometric methods, pathfinding algorithms (A*), combinatorial optimisation or metaheuristics [8]. Flight plan optimisation fits well this category as the network of routes, in its traditional or Free Route version can naturally be modelled with a graph. New contributions are often formulated with the definition of different cost functions, addressing fuel consumptions and emissions [9], persistent contrails [7], [10], [11], radiative

forcing [12], or global warming potential (GWP) [13]. Some determine a multi-criteria cost function considering an aggregation of fuel consumption, flight duration and flown distance [14]. Some trajectory optimisation algorithms used with real time weather conditions permit the avoidance of significant meteorological effects [15].

In this contribution, we do not address contrail formation but focus on CO_2 and non-CO_2 emissions, of which can be computed based on an estimation of the fuel flow along the trajectory and weather forecast. Going for a graph-based approach enables us to not focus on particular properties of the mathematical equations (continous, linear, differentiable, etc.) behind physical quantities needed to be computed for each edge of the graph. Different approaches for constructing the graph exist, e.g. the 3D graph construction described in [9]. Tian et al. [16] consider separately vertical and horizontal graphs and execute a different optimisation on each of them. Others consider a grid over a map, optimise a path and match a route a posteriori [17].

Our proposed approach has been tested on different scenarios extracted from real life conditions in December 2021, covered by AIRAC cycle 2112 (from December 2nd to 29th). Atmospheric conditions taken into account are extracted from the latest known forecast at the actual off-block time (AOBT) of the trajectory. Latest actual filed flight plans and optimised flight plans were then compared and yielded consistent trends in the route and altitude choices that were made. As cost indexes chosen by airlines to optimise their profit are bound to remain unknown, we do not aim at a point to point comparison, which would not make sense in this context.

The key contribution of the paper lies in the implementation details of the A* algorithms, which keeps the number of visited nodes low and yields a decent solution in an acceptable computation time. In some situations, the method shows promising results, with a reduction in fuel, CO_2 and NO_X emissions of 5 % for a medium haul flight in Europe (here Rome to Helsinki).

In Section II we detail the data sources we consider for network information, wind data, aircraft performance and emission models. Section III goes into detail on our methodology, and results are presented in Section IV. Impact and limitations are discussed in Section V and in the Conclusion.

II. Sources of data

A. Flight plan data

Flight plans consist of information about the intended route for an aircraft flying from an origin to a destination airport. They contain information about altitudes, speed and segments the aircraft intends to fly. For instance, a Toulouse LFBO to Paris–Orly LFPO flight plan could look like `N0385F280 FISTO5B FISTO UY156 PERIG UT210 TUDRA UT158 AMB AMB9W`; the aircraft departs Toulouse with the FISTO5B Standard Instrument Departure (SID) procedure until FISTO where it plans to reach Flight Level (FL) 280, i.e. 28,000 ft, and fly at 385 kts. It will follow airway UY156 to PERIG, airway UT120 to TUDRA, airway UT158 to AMB before following the Standard Terminal Arrival (STAR) procedure AMB9W to Paris–Orly.

An airway is defined by a succession of waypoints. For example, route UT158 goes through CNA, TUDRA, BEVOL, AMB, DIBES, etc. When a flight plan reads `TUDRA UT158 AMB`, it is implied it goes through all waypoints on UT158 between the two references, here `TUDRA-BEVOL-AMB`. Direct instructions DCT may be encoded in place of the route if the aircraft will not follow any additional waypoints.

The Free Route concept allows aircraft to not follow any ARN airway in a free route area (FRA); aircraft must however enter and exit the area through designated points and should follow usual routes outside these areas. Information about FRA also comes out of the AIRAC description files. These consist of airspace definitions (Figure 1) and waypoints associated with a FRA (Figure 2), of type:

- Entry (E), exit (X) of airspace or both (EX), located on the sides of the airspace polygon;
- Intermediate (I) points;
- Arrival (A), departure (D) or both (AD). This nomenclature is always associated to one or more airports.

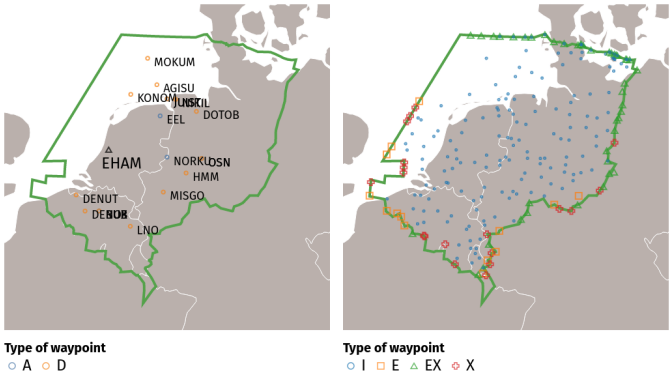

Fig. 2. Waypoints associated with Amsterdam–Schiphol airport EHAM and Maastricht Upper Area Control MUAC_FRA

B. Network data

All information about waypoints, ATS route network (ARN) and free route areas are extracted from official description files of the AIRAC 2112 cycle (December 2 to 29). Data consists of XML files following the AIXM standard and produced by Eurocontrol. We downloaded these files from Eurocontrol Network Manager B2B web services. You have to own a B2B certificate granted by Eurocontrol to get access to this data. Similar information in a different format is also accessible through the DDR service.

C. Atmosphere model

The atmosphere model is based on data provided by Météo France [18]. Météo France runs different atmospheric models to examine and predict the evolution of the atmosphere on different geographical domains at different levels and time horizons. The ARPEGE model provides different forecast parameters in the form of horizontal regular grids of $0.1° \times 0.1°$ for Europe and $0.5° \times 0.5°$ for the whole world. Vertically, the European ARPEGE parameters are defined at 23 different levels from 100 hPa to 1000 hPa. 100 hPa corresponds to a pressure altitude of 53 000 ft in the International Standard Atmosphere (ISA) model. Different time horizons are provided between 0 h and 114 h. Finally, runs are regularly generated, generally every 6 hours.

In our study, we consider the last known forecast with pressure, temperature and zonal and meridional (u and v) components of the wind. For each aircraft position, each parameter is bilinearly interpolated in the plane, then vertically and time-interpolated. Components of the wind are combined to determine its strength and its direction.

D. Fuel flow model

The BADA (version 3) aircraft performance model is used in the paper to derive fuel flow at different flight conditions. BADA 3 models fuel flow as a function that is primarily dependent on the aircraft speed and total net thrust:

$$\mathsf{ff} = C_{\mathrm{fcr}} \cdot \eta \cdot T \tag{1}$$

where η is the thrust specific fuel consumption, T is the total engine thrust, and C_{fcr} is a constant and engine specific cruise fuel flow factor. For jet engines, the thrust specific fuel consumption is calculated as:

$$\eta = C_{\mathrm{f1}} \left(1 + \frac{V}{C_{\mathrm{f2}}}\right) \tag{2}$$

where V is the true airspeed. C_{f1} and C_{f2} are constant coefficients and specific for each aircraft type.

In the point-mass performance model, during the cruise phase of the flight, the thrust is considered to be equal to the total drag of the aircraft as the flight states are relatively constant. The actual net thrust is further calculated based on the drag polar model, specifically, as:

$$\begin{aligned} T = D &= C_D \cdot \frac{1}{2}\rho V^2 S \\ &= (C_{\mathsf{D0}} + kC_L^2) \cdot \frac{1}{2}\rho V^2 S \\ &= \left[C_{\mathsf{D0}} + k \left(\frac{mg}{\frac{1}{2} \cdot \rho V^2 S} \right)^2 \right] \cdot \frac{1}{2}\rho V^2 S \end{aligned} \tag{3}$$

where C_{D0}, k are drag polar coefficients. ρ is the air density that is derived from aircraft barometric altitude. S is the wing surface area. Combining all three components together, we have the final model for fuel flow:

$$\mathsf{ff} = C_{\mathsf{fcr}} C_{\mathsf{f1}} \left(1 + \frac{V}{C_{\mathsf{f2}}} \right) \cdot \left[C_{\mathsf{D0}} + k \left(\frac{2mg}{\rho V^2 S} \right)^2 \right] \cdot \frac{1}{2}\rho V^2 S \tag{4}$$

From the previous equation, in BADA 3 model, the performance variables affecting fuel flow are aircraft mass (m), speed (V), temperature and altitude (related to air density ρ in the equation). These parameters are to be considered by the flight plan optimiser.

E. Emission model

Based on the fuel flow, the emissions are calculated with OpenAP [5]. It provides the necessary baseline engine performance and emission calculation based on ICAO emission databank. Emissions, including CO_2, $SO_X$and H_2O, are linear with the fuel flow, which is shown in Table I, where the emission index gives the mass of emission per mass of fuel burnt across all aircraft and engine types.

TABLE I
CONSTANT EMISSION INDEX

Emission	Emission Index (EI)
CO_2	3140 g / kg fuel
water vapor	1230 g / kg fuel
SO_2	0.84 g / kg fuel

The emission models for NO_X, CO and HC are not linearly related to the fuel flow. OpenAP implements corrections models based on Boeing Fuel Flow Method 2 [19]. Finally, all emission types can be calculated based on the aircraft flight conditions (altitude and speed) and related performance parameters (mass and fuel flow).

F. Climate cost model based on emissions

The climate impact of a trajectory is partly based on different emissions from aircraft. Lee et al. identify carbon dioxide (CO_2), nitrogen oxides (NO_X), water vapor, soot and sulfate (SO_2) [1].

Currently, different metrics exist for calculating the contribution of aviation to climate change, which are global warming potential (GWP) and global temperature change potential (GTP). These metrics are often presented at three time horizons, which are 20, 50 and 100 years. GWP corresponds to the heat absorbed by a gas, relative to the heat absorbed by the same mass of CO_2. By definition, the GWP of CO_2 is 1. Table II gives the latest known corresponding CO_2-equivalent emissions for the different aforementioned gases [1].

NO_X emissions induce a lot a chemical reactions in the atmosphere [20]. Depending on different conditions, NO_X may have positive or negative impacts on global warning [1]. Lee et al. propose average emission indexes to calculate NO_X's contribution (Table III).

TABLE II
GWP CO_2-EQUIVALENT EMISSIONS

GWP metric	$\mathbf{GWP_{20}}$	$\mathbf{GWP_{50}}$	$\mathbf{GWP_{100}}$
CO_2	1	1	1
NO_X	619	205	114
water vapor	0.22	0.10	0.06
soot	4288	2018	1166
SO_2	-832	-392	-226

TABLE III
AVERAGE EMISSION INDEX

Emission	Emission Index (EI)
NO_X	15.14 g / kg fuel
soot	0.03 g / kg fuel

Based on constant and average Emission Indexes, we can define a climate change cost function :

$$\mathsf{cost(t)} = \sum_{i=1}^{n_{\mathsf{gas}}} \mathsf{GWP}_i \cdot \mathsf{EI}_i \cdot \int_{t_0}^{t_f} \mathsf{ff}(t)\, dt \tag{5}$$

where GWP_i is the CO_2-equivalent emission (see Tables I and III), EI_i the emission index for the i-th gas (see Table II) and $\mathsf{ff}(t)$ the fuel flow (Section II-D).

III. METHODOLOGY

A. Problem definition

Our problem consists in finding the optimum path between a departure and an arrival airport. It can be assimilated to a shortest path problem in a graph G. G can be defined by the pair (V, E), where V represents the set of nodes (in our case, the set of waypoints and airports at different altitudes) and E the set of edges. In a fixed route network, these edges correspond to the airways connecting different en-route waypoints and connections between airports and en-route phase of flight represented by the standard procedures of arrival and departure. In a Free Route network, they correspond to all the possible connections between Free Route waypoints and airports connected to the Free Route network.

Any node $V_i \in V$ is defined by a triplet (latitude, longitude, altitude) that represents a waypoint at a specific altitude. Any element of the set E is a triplet $(V_i, V_j, c_{i\to j})$ directly connecting two nodes of the graph V_i and V_j. $c_{i\to j} \in \mathbb{R}$ represents the cost to go from V_i to V_j. We denote by V_0 the starting node or departure airport and V_n the final node or arrival airport.

We can also define on G a path to go from a node V_i to another one V_j, as a list of edges to follow:

$$\gamma_{i\to j} = (e_1, ..., e_n) \in \mathbf{E}^n \tag{6}$$

The nodes V_i and V_j are not necessarily directly connected, but a path must follow the constraints of the airspace network :

$$\forall i \in [0, n-1] \quad e_i \text{ is directly connected to } e_{i+1} \tag{7}$$

We also denote by $V_i \to V_j$ a `DIRECT` between the nodes V_i and V_j. A `DIRECT` does not necessarily follow the constraints of the airspace network and allows to go directly from V_i to V_j.

The cost associated with a path γ is given by the following equation

$$f(\gamma) = \sum_{e_i \in \gamma} c(e_i) \tag{8}$$

where $c(e_i)$ is the cost associated to an edge $e_i \in E$.

A shortest path problem on a graph consists in solving the problem $\min_\gamma f(\gamma)$ to find a path γ from V_0 to V_n minimising the cost function f. The Dijkstra algorithm is a well-known algorithm to solve such a problem. It consists of a Breadth-First Search (BFS) of the graph G: nodes are explored in such a way that all explored nodes at a given step are reachable with a partial cost smaller than the cost required by path until the latest explored node. In this way, it guarantees the identification of a solution if it exists. However, the time complexity of such an algorithm can be very important [21].

The A* algorithm is an extension of the Dijkstra algorithm where a heuristic guides the search towards the most promising nodes. At each iteration, it selects nodes which minimise the function

$$f(V_0..V_n) = g(V_0..V_i) + h(V_i..V_n) \tag{9}$$

where $g(V_0..V_i)$ is the cost from the starting node to the current node and $h(V_i..V_n)$ an heuristic that estimates the cost to go from the current node to the final node. The quality of the result depends on the quality of the chosen heuristic. An heuristic is said to be *admissible* when it never overestimates the cost to reach the final node. In this case, the found solution is optimal. An heuristic is said to be *consistent* when

$$h(V_i..V_n) <= g(V_i..V_{i+1}) + h(V_{i+1}..V_n) \tag{10}$$

In this case, it guarantees that once a node is expanded, the cost to reach this node is minimal. A consistent heuristic is admissible. In the following, we detail how A* was adapted to solve our problem.

B. Adaptations

1) Exploration cone: At each iteration, the A* algorithm selects the most promising node, i.e. the one with the lowest f. Then, it expands each neighbour of this node by assessing the associated cost and heuristic values. In our problem, this assessment needs an evaluation of the flight model. However, as neighbour nodes heading in the opposite direction of the current flight direction are clearly of no value for our search, we should not evaluate the cost and heuristic associated to these nodes and to their associated subtree.

Removing nodes from the expansion phase limits the number of calls to the flight model. Thus, we define an exploration cone limiting the number of neighbour nodes to be actually assessed. Specifically, the exploration cone (Figure 3) only includes waypoints that would cause a small heading change. The cone is defined with an initial opening angle (typically 30°). This angle may be increased when no points are found, e.g. around the arrival airports, when there are few points left to compute the final part of the trajectory. Finally, points remaining in the cone are clustered to prune those that are close to each other.

2) Cost functions: A* algorithm needs a cost function g to assess the cost to go from a node V_i to a node V_{i+1}. Different functions may be considered, e.g. the great-circle distance to find the shortest path, or the fuel to burn between V_i and V_{i+1}, or further, CO_2 and non-CO_2 emissions.

In Section II-F, we introduce a Climate Cost Function based on emissions. Apart from the great-circle distance, these different cost functions depend on fuel flow. As fuel flow depends on the mass of the aircraft and mass varies significantly along the trajectory, the calculated fuel flow at a node depends on all past nodes, and not only the previous point as usually presented in shortest-path problems. Therefore, it is important to note that for any cost functions based on fuel flow, $g(V_i..V_{i+1})$ may differ according to the path to reach V_i. Different strategies like topological sort or backtracking exist to address this issue. Finally, our cost function g could be rewritten as a past-dependent cost function :

$$g(V_{i-1}..V_i+1) = g(V_i)_{V_0...V_{i-1}} = c(V_0...V_i) - c(V_0...V_{i-1}) \tag{11}$$

where:

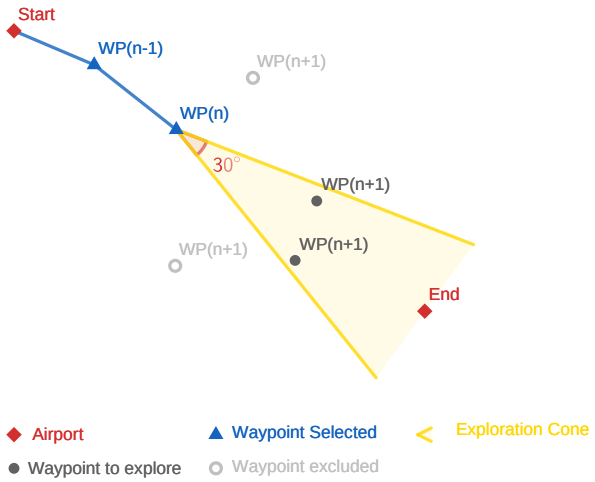

Fig. 3. The exploration cone limits the number of nodes to explore.

- $c(V_0...V_i)$ is the cost to reach the current node V_i from the departure node V_0, e.g., the total fuel consumption until V_i,
- $c(V_0...V_{i-1})$ is the cost to reach the previous node V_{i-1} from the departure node V_0.

3) Heuristic: We define our heuristic such as:

$$h(V_i...V_n) = \alpha \cdot c(V_i \rightarrow V_n) \tag{12}$$

where:

- $\alpha \in [0, 1]$. If $\alpha = 0$, A* behaves like a Dijkstra algorithm.
- $c(V_i \rightarrow V_n)$ is the cost to reach the final node V_n with a `DIRECT` instruction.

A `DIRECT` does not respect the network constraints, but it ensures, without wind, that the cost estimation is always lower than the real cost. α is sufficiently small to ensure that the heuristic function h remains *admissible* in all weather conditions, but not too small to discourage the selection of nodes of less importance.

4) Neighbour selection: In a fixed route network, one cannot go from any waypoint to any waypoint, no matter how close they are. Neighbouring nodes are selected according to the airways connecting them. Some of these points correspond to SID or STAR and allow the connection between the route network and the different airports.

In a Free Route network, the neighbouring nodes are selected according to the following rules :

- Each airport is connected to several departure points.

$$\forall d \in \mathcal{D}\ \forall\, p \in \mathcal{P}(d) \quad p \hookrightarrow d$$

- Each arrival point is connected to an airport.

$$\forall a \in \mathcal{A}\ \forall\, p \in \mathcal{P}(a) \quad a \hookrightarrow p$$

- A flight can go from an entry point to an exit point.

$$\forall f \in \mathcal{F}\ \forall e \in \mathcal{E}(f)\ \forall x \in \mathcal{X}(f) \quad e \hookrightarrow x$$

- A flight can go from a departure point to an exit point.

$$\forall f \in \mathcal{F}\ \forall d \in \mathcal{D}\ \forall x \in \mathcal{X}(f) \quad d \hookrightarrow x$$

- A flight can go from an entry point to an arrival point.

$$\forall f \in \mathcal{F}\ \forall e \in \mathcal{E}(f)\ \forall a \in \mathcal{A} \quad e \hookrightarrow a$$

where $\mathcal{F}$ is the set of Free Route areas, $\mathcal{E}(f)$ the set of entry points in the FRA f, $\mathcal{X}(f)$ the set of exit points in the FRA f, $\mathcal{D}$ the set

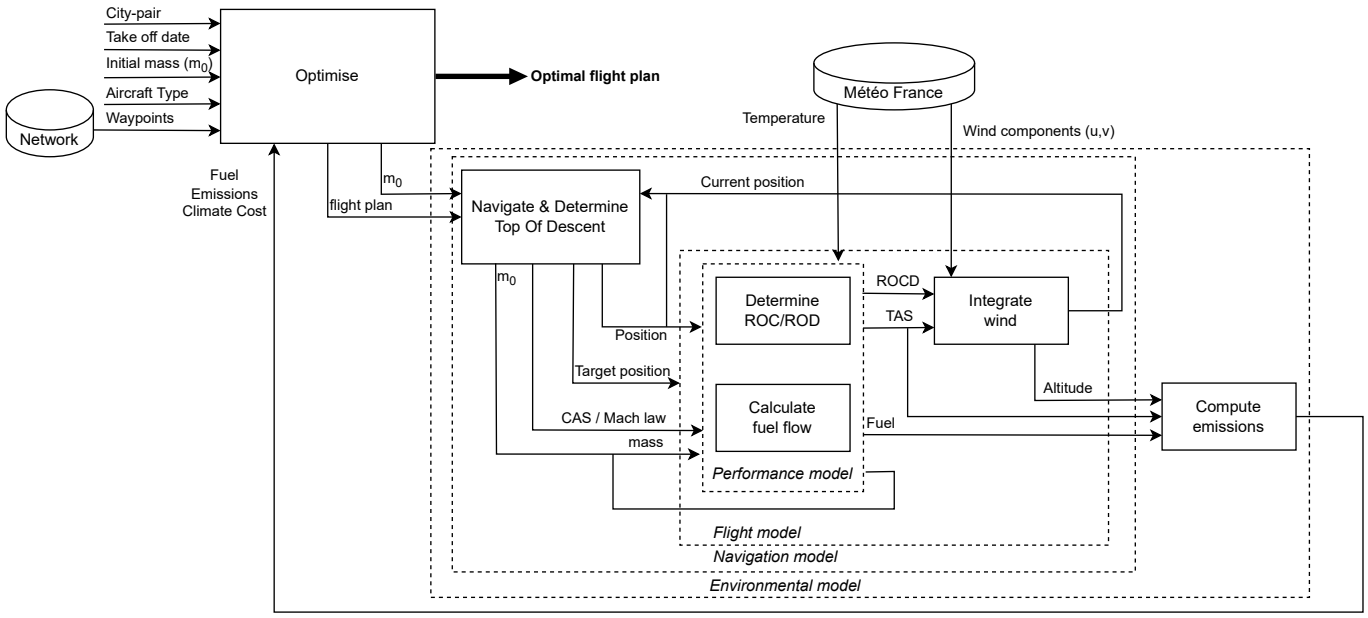

Fig. 4. Optimisation global overview

of Departure points, $\mathcal{A}$ the set of Arrival points and $\mathcal{P}(e)$ the set of airports associated to the Departure or Arrival point e. $V_i \hookrightarrow V_j$ represents a directed edge from V_i to V_j.

Moreover, it is useless to expand exit points when an arrival point connected to the final airport is found.

C. Implementation

A global overview of our implementation is presented in Figure 4. The optimiser determines a flight plan to be simulated based on the following inputs : origin and destination airports, departure date (EOBT), aircraft type and initial mass. A navigation model determines the Top of Descent and the different target positions to reach.

For each target position, a flight model determines the True Air Speed (TAS) and the required Rate Of Climb/Descent (ROC/ROD) to reach the position. The throttle is set to maximum climb thrust during both take-off and climb phases or idle thrust during descent [22]. During cruise, thrust is set equal to drag. TAS is set according to the recommended speed procedures for climb, cruise and descent phases from BADA [22]. Once thrust and TAS are known, ROC/ROD is calculated using the energy share factor principle. The energy share factor determines how power is allocated to climb and acceleration. Temperature, used to calculate air density, is read into GRIB files provided by Météo France (Section II-C). Once ROC/ROD and TAS are known, wind is also obtained from GRIB files to determine the ground speed and new position of the flight. Mass is updated according to the associated fuel flow (Section II-D). This process is repeated until the target position is reached and then the final position. Lastly, an environmental model calculates the emissions and returns them to the optimiser.

Our implementation is based on the graph library GraphStream [23]. GraphStream implements different shortest-path algorithms. Each algorithm takes a graph as input. In our study, this graph is initialised with two nodes : the starting and final nodes. At first, no edge is added. As the A* algorithm proceeds with the exploration (Section III-A), nodes and edges are dynamically added to the graph. When a node is expanded, different simulations for each interesting neighbour nodes (Sections III-B1 and III-B4) are run in parallel. Each simulation yields a flight plan starting from the current node V_i, going to a neighbour node V_{i+1} and then to the final node V_n. The segment $V_i..V_{i+1}$ is used to determine the cost value g (Section III-B2), whereas the segment $V_{i+1} \rightarrow V_n$ is used to determine the heuristic value h (Section III-B3).

D. Assumptions

The framework relies on different assumptions. 1) Aircraft cruise at a constant Mach number all along the trajectory. 2) Parity, that may induce a change level, are not taken into account. 3) In the Free Route network, intermediate points are not considered. 4) Forbidden zones, turbulence areas, approach and departure procedures are ignored. 5) Contrail cirrus are not taken into consideration in this paper.

IV. Experiments

A. Use cases

This section presents the results of our optimisation method for different test cases. We consider real flight plans that were filed in December 2021. As the Free Route Environment only contains en-route points, SID and STAR are not taken into consideration. The last point of a SID is assimilated to a Departure point and the first point of a STAR to an Arrival point. Between these points and airports, we simulate a `DIRECT`.

We considered a set of flights plans from *Roma–Leonardo da Vinci* airport in Italy (`LIRF`) to *Helsinki–Vantaa* airport in Finland (`EFHK`). Figure 5 presents on the left hand side all the different flights plans that were filed in December 2021. The large range of trajectories spans over a wide area, roughly between West Austria and Hungary, then between West and East Poland. It also ensures that the result of our optimisation should find trajectories which lies entirely within Free Route Areas existing at this moment (Figure 1).

We consider more specifically two flights that were operated by an A319 aircraft. The first one, Aircraft A, took off on December 1st (Middle top of Figure 5). Its route was `M079F390 TIBER DCT NIKOL DCT PUL DCT GIRDA DCT TIVAP DCT UPEGU DCT LEGAZ DCT TOMTI DCT DIMEX DCT KUNER DCT OLMOR DCT BALIT DCT KEDUX DCT LOGNA DCT LONSA DCT SORPA DCT INTOR`. The second one, Aircraft B, took off on December 20th (Right top of Figure 5). Its `ICAO` route is `M079F380 OKUNO DCT ATRUP DCT TORPO/M079F390 DCT KOPRY`

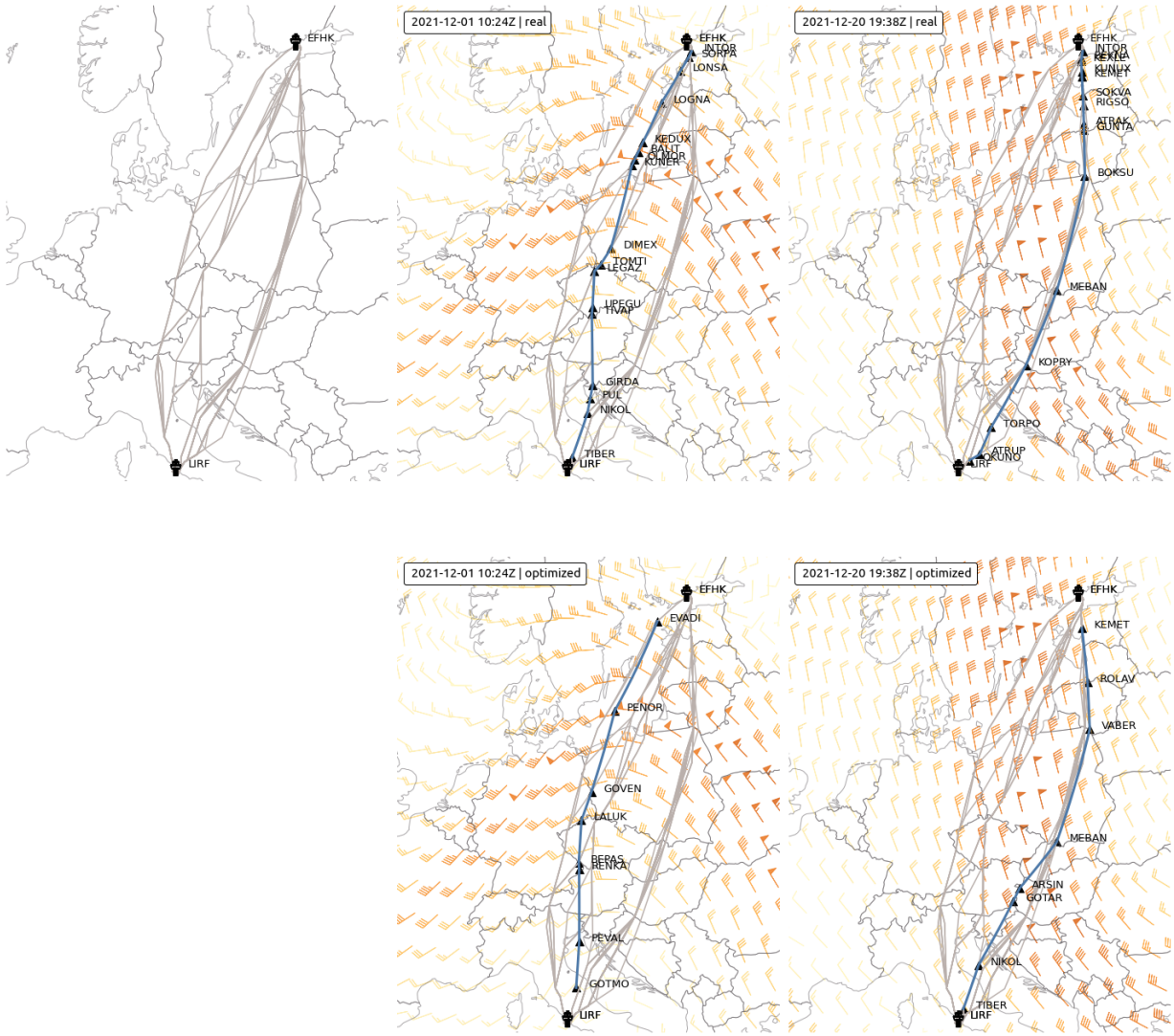

Fig. 5. Real and optimised flight plans between Roma Leonardo da Vinci LIRF and Helsinki Vantaa EFHK airports. All filed flight plans in December 2021 are plotted on the top left-hand corner. Then, we picked two days with different atmospheric conditions to illustrate different optimum resulting flight plans.

DCT MEBAN DCT BOKSU DCT GUNTA DCT ATRAK DCT RIGSO DCT SOKVA DCT KEMET. In both cases, the cruise Mach number is assumed to be 0.79, which is a classic operating speed for A319.

The optimiser is configured to search for optimal flights plans between LIRF and EFKH, with the same aircraft type. The flight level range is set between FL310 and FL410, which is the highest altitude that can be reached with an A319. The initial mass is set to the reference mass given by the BADA model. The initial size of the exploration cone is set to 60°. We limit the distance between two expanded waypoints to 10 NM.

The shortest-distance flight plan filed in December 2021 is taken as a reference to which compare the results of our optimisation. It results from a similar optimisation with great-circle distance cost. In the case of the city pair LIRF-EFHK, it corresponds to the route KATAR DCT BAXON DCT MIKOV DCT DESEN DCT RANOK DCT TIGNU DCT GARSO DCT EVADI.

B. Results

For Aircraft A, the optimisation returns the flight plan M079F410 TIBER DCT SOVOX DCT LAMSI DCT BEPAS DCT LALUK DCT POGAB DCT SUBIX DCT PENOR DCT EVADI. Aircraft B gets a second flight plan M079F410 KATAR DCT IBENI DCT GOTAR DCT SKARY DCT BOKSU DCT ASKOR DCT KEMET. The corresponding routes are represented at the bottom of Figure 5. Both trajectories are quite similar to the real ones. In particular, Aircraft B exploited weather conditions to limit the impact of head winds.

In Table IV and V, we calculate different metrics to compare the results of our optimisation to other flight plans :

- *Flight time*: the duration of the flight ;
- *Flown distance*: the distance covered by the flight ;

- *RFL, Requested Flight Level*: the highest Flight Level required in the flight plan;
- *Fuel*: the fuel burnt according to the BADA model ;
- *CO_2*: CO_2 emitted according to the OpenAP model ;
- *NO_X*: NO_X emitted according the the OpenAP model ;
- *CCF*: an assessment of the Climate Impact as presented in Section II-F, page 3, with constants from GWP_{20}.

These different metrics are compared between the reference flight plan (the shortest distance), the real flight plan (one that has been actually filed and flied in these actual conditions), and our optimised flight plan. To better compare the results, we introduce a fourth flight plan, which is the optimised flight plan flying at a lower altitude.

By definition, the reference flight plans are the shortest-distance flight plans. In atmospheric conditions equivalent to the real ones, they spend more time in air, consume more fuel and emit more. The optimised flight plans shows significant improvements in terms of flight time, fuel consumption and emissions. They also yield better metrics than for actual trajectories.

However, the optimiser systematically suggests to fly at a higher flight level. Even if Aircraft B benefits from milder head wind, gains are primarily due to flight level change. In comparison, the fourth flight plan shows only slight improvements, even at the same altitude (see Column Opt_{390}).

TABLE IV
AIRCRAFT A – METRICS

	Reference	**Real**	**optimised**	**Opt_{390}**
Flight time (s)	10585	10524	**10123**	10350
Flown distance (NM)	**1238**	1250	1244	1244
RFL	**390**	**390**	410	**390**
Fuel (kg)	5850	5816	**5593**	5727
CO_2 (t)	18.4	18.3	**17.6**	18.0
NO_X(kg)	57.8	57.5	**56.0**	56.7
CCF (t CO_2 eq)	69.8	69.4	**66.8**	68.4

TABLE V
AIRCRAFT B – METRICS

	Reference	**Real**	**optimised**	**Opt_{390}**
Flight time (s)	11986	11738	**11269**	11720
Flown distance (NM)	**1238**	1260	1257	1257
RFL	**390**	**390**	410	**390**
Fuel (kg)	6586	6467	**6196**	6453
CO_2 (t)	20.7	20.4	**19.5**	20.3
NO_X(kg)	64.2	63.2	**61.3**	63.0
CCF (t CO_2 eq)	78.6	77.2	**74.0**	77.0

Table VI presents the performance of the algorithm. The reference column corresponds to the case without wind. The cone significantly limits the number of expanded nodes and consequently the number of calls to the flight model. The clustering inside the cone limits the number of neighbour nodes that are expanded for each node (on average about 4 edges per node); it avoids expanding nodes that are very close to each other. Furthermore, wind conditions on December 1st (aircraft A) and December 20th (aircraft B) further help to reduce the number of explored nodes.

TABLE VI
EFFECT OF WIND ON EXPLORATION PERFORMANCE

	Aircraft A	**Aircraft B**	**Reference**
Expanded nodes	159	171	210
Expanded edges	717	656	1157
Ratio	4.5	3.8	5.5

V. DISCUSSION

A* appears to be a viable deterministic solution to perform 3D flight plan optimisation, in a fixed route or free route network (in spite of the combinatory explosion brought by free route areas), provided that we efficiently prune the search space. Techniques such as the exploration cone introduced in the Methodology section allowed us to do without stochastic methods and metaheuristics, making our method easier to implement in an operational context where convergence and correction guarantees may be expected.

In more advanced versions of our implementation, we expect an increase of the search space size by taking speed into account. The risk, in particular with speed considerations, is that the A* algorithm explores many edges and subpaths yielding very similar costs. The key to the A* exploration remains an efficient pruning of the search space which limits the number of calls to the performance model.

Differences between the results of the optimisation and actual filed flight plans often dependent on the chosen flight level, which raises more questions about how we modelled aircraft capabilities; aircraft physics, operational constraints or common ATC practices may explain why aircraft do not fly at their optimal flight level. In practice, it is actually unfeasible to let all aircraft fly at their optimal altitude and compromises must be considered to equally share the burden among airspace users.

We consider room for improvement in terms of aircraft performance modelling capabilities and in terms of algorithms. We could, for example, consider a first coarse lateral optimisation of flight plans, followed by local optimisations to adjust speed and altitude and further optimise good quality flight plans. However, these further optimisations may be counterbalanced by the uncertainty inherent to the problem and conditions in which aircraft fly, in terms of wind, operational constraints, ATC decisions or human factors.

VI. CONCLUSION

This paper presents the details of the implementation of an A* algorithm designed to optimise flight plans with environmental constraints (fuel consumption, CO_2 and non-CO_2 emissions), taking operational constraints (fixed route and free route networks) and weather forecasts into account. With proper optimisations, the search space becomes small enough so that the deterministic algorithm returns optimal trajectories in a reasonable time (within a minute of computation on a standard laptop computer).

While preliminary results are promising, the authors consider the following improvements for future works, including a better modelling of cost indexes for airlines, the ability to change speed and flight levels halfway through the flight plan, the ability to fly around areas of interests (military areas, turbulence areas) and improved environmental considerations in the cost function, e.g. taking contrail formation into account.

DISCLAIMERS

This document has been created with elements of Base of Aircraft Data (BADA) Family 3 Release 3.15 which has been made available by EUROCONTROL to ONERA. EUROCONTROL has all relevant rights to BADA.

REFERENCES

[1] D. Lee, D. Fahey, A. Skowron, M. Allen, U. Burkhardt, Q. Chen, S. Doherty, S. Freeman, P. Forster, J. Fuglestvedt, A. Gettelman, R. De Len, L. Lim, M. Lund, R. Millar, B. Owen, J. Penner, G. Pitari, M. Prather, R. Sausen, and L. Wilcox, "The contribution of global aviation to anthropogenic climate forcing for 2000 to 2018," *Atmospheric Environment*, vol. 244, p. 117834, 2021.

[2] R. Chai, A. Savvaris, A. Tsourdos, S. Chai, and Y. Xia, "A review of optimization techniques in spacecraft flight trajectory design," *Progress in Aerospace Sciences*, vol. 109, no. 100543, 2019.

[3] V. Williams and R. B. Noland, "Variability of contrail formation conditions and the implications for policies to reduce the climate impacts of aviation," *Transportation Research Part D: Transport and Environment*, vol. 10, no. 4, pp. 269–280, 2005.

[4] A. Nuic, D. Poles, and V. Mouillet, "BADA: An advanced aircraft performance model for present and future ATM systems," *International Journal of Adaptive Control and Signal Processing*, vol. 24, pp. 850–866, Aug. 2010.

[5] J. Sun, J. M. Hoekstra, and J. Ellerbroek, "OpenAP: An Open-Source Aircraft Performance Model for Air Transportation Studies and Simulations," *Aerospace*, vol. 7, p. 104, July 2020.

[6] S. Matthes, V. Grewe, K. Dahlmann, C. Frömming, E. Irvine, L. Lim, F. Linke, B. Lührs, B. Owen, K. Shine, S. Stromatas, H. Yamashita, and F. Yin, "A concept for multi-criteria environmental assessment of aircraft trajectories," *Aerospace*, vol. 4, p. 42, Aug 2017.

[7] M. Soler, B. Zou, and M. Hansen, "Flight trajectory design in the presence of contrails: Application of a multiphase mixed-integer optimal control approach," *Transportation Research Part C: Emerging Technologies*, vol. 48, pp. 172–194, 2014.

[8] A. Murrieta-Mendoza and R. M. Botez, "Commercial aircraft trajectory optimization to reduce flight costs and pollution: Metaheuristic algorithms," in *Advances in Visualization and Optimization Techniques for Multidisciplinary Research*, pp. 33–62, Springer, 2020.

[9] C. Ramée, K. Junghyun, M. Deguignet, C. Justin, S. Briceno, and D. N. Mavris, "Aircraft flight plan optimization with dynamic weather and airspace constraints," 2020.

[10] Y. Lim, A. Gardi, M. Marino, and R. Sabatini, "Modelling and evaluation of persistent contrail formation regions for offline and online strategic flight trajectory planning," in *Sustainable Aviation*, pp. 243–277, Springer, 2016.

[11] D. Xue, K. K. Ng, and L.-T. Hsu, "Multi-objective flight altitude decision considering contrails, fuel consumption and flight time," *Sustainability*, vol. 12, no. 15, p. 6253, 2020.

[12] Y. Lim, A. Gardi, and R. Sabatini, "Optimal aircraft trajectories to minimize the radiative impact of contrails and CO2," *Energy Procedia*, vol. 110, pp. 446–452, 2017. 1st International Conference on Energy and Power, ICEP2016, 14-16 December 2016, RMIT University, Melbourne, Australia.

[13] J. S. Fuglestvedt, K. P. Shine, T. K. Berntsen, J. Cook, D. S. Lee, A. Stenke, R. B. Skeie, G. J. M. Velders, and I. A. Waitz, "Transport impacts on atmosphere and climate: Metrics," *Atmospheric Environment*, vol. 44, pp. 4648–4677, 2010.

[14] J. Rosenow, D. Strunck, and H. Fricke, "Trajectory optimization in daily operations," *CEAS Aeronautical Journal*, vol. 11, no. 2, pp. 333–343, 2020.

[15] S. Alam, H. A. Abbass, and M. Barlow, "Multi-objective ant colony optimization for weather avoidance in a free flight environment," *The Artificial Life and Adaptive Robotics Laboratory, University of New South Wales, Canberra, Australia*, 2006.

[16] Y. Tian, X. He, Y. Xu, L. Wan, and B. Ye, "4D trajectory optimization of commercial flight for green civil aviation," *IEEE Access*, vol. 8, pp. 62815–62829, 2020.

[17] S. Samolej, G. Dec, D. Rzonca, A. Majka, and T. Rogalski, "Regular graph-based free route flight planning approach," *Aircraft Engineering and Aerospace Technology*, vol. 93, pp. 1488–1501, Nov. 2021.

[18] "Public data portal from Météo France." https://donneespubliques.meteofrance.fr/. Accessed: 2022-02-11.

[19] D. DuBois and G. C. Paynter, "Fuel Flow Method2 for estimating aircraft emissions," *SAE Transactions*, pp. 1–14, 2006.

[20] J. van Manen and V. Grewe, "Algorithmic climate change functions for the use in eco-efficient flight planning," *Transportation Research Part D: Transport and Environment*, vol. 67, pp. 388–405, 2019.

[21] A. R. Soltani, H. Tawfik, J. Y. Goulermas, and T. Fernando, "Path planning in construction sites: performance evaluation of the Dijkstra, A-star, and GA search algorithms," *Advanced engineering informatics*, vol. 16, no. 4, pp. 291–303, 2002.

[22] "User Manual for the Base of Aircraft Data (BADA) Revision 3.15," tech. rep., Eurocontrol, 2019.

[23] A. Dutot, F. Guinand, D. Olivier, and Y. Pigné, "GraphStream: A Tool for bridging the gap between Complex Systems and Dynamic Graphs," in *Emergent Properties in Natural and Artificial Complex Systems. Satellite Conference within the 4th European Conference on Complex Systems (ECCS'2007)*, (Dresden, Germany), Oct. 2007.